Chang, Yunhua; Zou, Zhong; Zhang, Yanlin; Deng, Congrui; Hu, Jianlin; Shi, Zhihao; Dore, Anthony J.; Collett, Jeffrey L. 2019. **Assessing contributions of agricultural and nonagricultural emissions to atmospheric ammonia in a Chinese megacity**. *Environmental Science & Technology*, 53 (4). 1822-1833. https://doi.org/10.1021/acs.est.8b05984

Assessing contributions of agricultural and non-agricultural emissions to atmospheric ammonia in a Chinese megacity

Yunhua Chang,[†, a] *Zhong Zou*, [‡, a] *Yanlin Zhang*,[†, *] *Congrui Deng*,[‡, *] *Jianlin Hu*,[△] *Zhihao Shi*,[△] *Anthony J. Dore*, [∥] *and Jeffrey L. Collett Jr.*[‡]

[†]Yale-NUIST Center on Atmospheric Environment, Nanjing University of Information Science & Technology, Nanjing 210044, China

[‡]Department of Environmental Science & Engineering, Institute of Atmospheric Sciences, Fudan University, Shanghai 200433, China

[△]School of Environmental Science and Engineering, Nanjing University of Information Science & Technology, Nanjing 210044, China

[∥]Centre for Ecology & Hydrology Edinburgh, Bush Estate, Penicuik, Midlothian EH26 0QB, UK

[♯]Department of Atmospheric Science, Colorado State University, Fort Collins, Colorado, 80523 USA

[a]Equally contributing co-authors

ABSTRACT Ammonia (NH_3) is the predominant alkaline gas in the atmosphere contributing to formation of fine particles - a leading environmental cause of increased morbidity and mortality worldwide. Prior findings suggest that NH_3 in the urban atmosphere derives from a complex mixture of agricultural (mainly livestock production and fertilizer application) and non-agricultural (e.g., urban waste, fossil fuel-related emissions) sources; however, a citywide holistic assessment is hitherto lacking. Here we show that NH_3 from non-agricultural sources rivals agricultural NH_3 source contributions in the Shanghai urban atmosphere. We base our conclusion on four independent approaches: (i) a full-year operation of a passive NH_3 monitoring network

at 14 locations covering urban, suburban, and rural landscapes; (ii) model-measurement comparison of hourly NH_3 concentrations at a pair of urban and rural supersites; (iii) source-specific NH_3 measurements from emission sources; and (iv) localized isotopic signatures of NH_3 sources integrated in a Bayesian isotope mixing model to make isotope-based source apportionment estimates of ambient NH_3. Results indicate that non-agricultural sources and agricultural sources are both important contributors to NH_3 in the urban atmosphere. These findings highlight opportunities to limit NH_3 emissions from non-agricultural sources to help curb $PM_{2.5}$ pollution in urban China.

1 Introduction

Atmospheric ammonia (NH_3) is the predominant alkaline gas in the atmosphere and actively involved in atmospheric chemistry. In reactions with sulphuric acid and nitric acid, formed via the oxidation of SO_2 and NO_x, respectively, NH_3 contributes to the formation of NH_4^+ salts, which typically make up from 20 to 80% of atmospheric

particulate matter with an aerodynamic diameter less than 2.5 micrometers ($PM_{2.5}$).[1-5] This fine particle formation has led to huge health and economic costs.[6-10]

There is an increasing importance of NH_3 emissions relative to SO_2 and NO_x worldwide due to relatively slow reduction of NH_3 emissons.[11-17] Over 90% of NH_3 emissions in China, the United States and many European countries result from agriculture, mainly including livestock production and NH_3-based fertilizer application;[6, 13, 15, 18-22] thus, agricultural NH_3 emissions are often blamed for high levels of ammonium-containing $PM_{2.5}$.[1, 6, 7, 23, 24] However, in urban areas where agricultural activities are mostly absent, a growing body of evidence suggests that non-agricultural activities like wastewater treatment,[25] coal combustion,[26] solid garbage,[27] vehicular exhaust,[28] and urban green space[29] also contribute to NH_3 emissions.[30] For example, large vehicular NH_3 emissions from noble metal-based three-way catalysts (TWCs) have been detected in chassis dynamometer vehicle experiments, road tunnel tests, and ambient air measurements dating back to the 1980s.[31-42] Nevertheless, Yao et al.[43] and Teng et al.[29] suggest that vehicular NH_3 emissions can be neglected and proposed

57 urban green spaces as the dominant contributor to urban atmospheric NH_3 in North
58 America and Northern China. There remains a long-standing and on-going controversy
59 regarding the relative contribution of agricultural and non-agricultural NH_3 emissions in
60 the urban atmosphere.[44-46]

61 In China, while there have been no long-term and nationwide NH_3 monitoring studies
62 like the U.S. passive Ammonia Monitoring Network (AMoN,
63 http://nadp.sws.uiuc.edu/amon) affiliated with the National Atmospheric Deposition
64 Program (NADP),[47-49] numerous researchers have measured NH_4^+ concentrations in wet
65 deposition (i.e., precipitation) for more than 30 years.[50, 51] The data show that the annual
66 flux of NH_4^+ in wet deposition in China has increased in conjunction with the growth in
67 animal production and fertilizer application.[17, 50, 52, 53] Further, China's recent economic
68 boom has been coupled with accelerated urbanization.[54, 55] In 1978 less than 20% of
69 Chinese residents lived in cities. The population of its cities has quintupled over the past
70 40 years, reaching 813 million or nearly 60% of the total population.[56] At present, there
71 are three super-regions or city clusters in China: the Pearl River Delta (PRD), next to

Hong Kong; the Yangtze River Delta (YRD), which surrounds Shanghai; and Jing-jin-ji (J^3), centered on Beijing.[57] In particular, the YRD region is arguably the most concentrated set of adjacent urban conurbations in the world.[58] Huge cities place huge demands on resource consumption and associated non-agricultural NH_3 emissions.[44] For example, the region has continuously experienced double-digit growth in auto sales since 2009.[36] The expanding motor vehicle population in its cities, in turn, is reshaping the urban atmospheric composition.[59, 60] Meanwhile, the vast rural areas of the YRD region are dominated by fluvial plains with fertile soil, and abundant production of rice and tea.[22] According to Huang et al.,[22] livestock production, N-fertilizer application, and non-agricultural sources (including sewage treatment, waste landfills, and human discharge) in the YRD region in 2007 comprise 48%, 40%, and 12% of the total 459 kt NH_3 emissions, respectively. The interplay of agricultural and non-agricultural NH_3 emissions in the region provides an ideal study area to investigate their impact on ambient NH_3 concentrations over time.

Taking Shanghai as an example, the present study aims to systematically elucidate the role of non-agricultural NH_3 emissions contributing to ambient NH_3 in the urban atmosphere through (1) investigating the spatial and temporal variability of NH_3 concentrations across various land use categories, (2) interpreting the consistency or discrepancy of NH_3 concentrations between field measurements and chemical transport model simulations, and (3) using stable isotopes as a tool to quantify source category contributions to ambient NH_3 concentrations in the rural and urban atmospheres.

2 Materials and methods

2.1 Site description

The Yangtze River Delta or YRD region encompasses the nation's largest population center, Shanghai, and major agricultural fields in eastern China. In order to obtain information regarding the spatial and temporal variability of NH_3 concentrations in Shanghai, we established a regional monitoring network of fourteen sites covering urban (FD, HK, YP, HP, PT, JA, LW, XH, and PD), suburban (ZJ and CJ), and rural (DH, SY and CM) landscapes (Fig. 1). Of particular importance are PD and DH, which

101 also serve as supersites intended to represent urban and rural settings, respectively. In
102 Shanghai, all ten state-control stations (SCS) of China's Ministry of Environmental
103 Protection were utilized. The advantages of selecting these SCS sites include (i) their
104 deliberate locations away from point and local sources of pollution, such as
105 transportation corridors, agricultural fields, livestock operations, and industrial
106 emissions; (ii) they have well-trained staff with long-term employment to sustain
107 continuous measurements; and (iii) they are equipped with refrigerators so that the
108 collected samples can be quickly stored to prevent potential contamination or sample
109 degradation. More detailed site descriptions can be found elsewhere.[36, 61] The
110 meteorology in Shanghai is typical of a subtropical monsoon system with four distinct
111 seasons. A summary of the average meteorological conditions can be found in SI Fig.
112 S1.

113 **2.2 Field sampling**

114 In order to obtain the spatial distributions of NH_3 concentrations over the Shanghai
115 region, from May 2014 to June 2015, weekly Ogawa PSDs (passive sampling devices,

Ogawa, FL, USA) were deployed at each site (from March 2017 to March 2018 for CM and SY sites) under the protection of an opaque shelter for collecting ambient NH_3. Between June and August of 2014, two Ogawa PSDs were deployed for monthly collection at the urban PD site and the rural DH site for N isotopic analysis of NH_3. The Ogawa PSD consists of a solid cylindrical polymeric body (2 cm diameter, 3 cm long) housing a citric acid-coated glass fiber disk at each end as a duplicate to trap NH_3.[48] All PSD components (including filters) were purchased from Ogawa USA, and sampling procedures provided by the manufacturer (http://www.ogawausa.com) were strictly followed throughout the campaign. After exposure, the filters were transferred with tweezers into plastic vials (15 mL) and stored at -18 °C immediately. The samples were delivered to the analytical laboratory monthly. The average relative percent difference between duplicate Ogawa PSD samples was 5.5%.

In order to relate temporal variations of NH_3 concentrations to potential NH_3 sources, the PD (urban) and DH (rural) sites were equipped with a Monitor for AeRosols and Gases (MARGA, Applikon B.V., NL), allowing continuous characterization of the

131 inorganic components of $PM_{2.5}$ (NH_4^+, NO_3^-, SO_4^{2-}, Cl^-, Na^+, K^+, Ca^{2+}, Mg^{2+}) and water-
132 soluble gases (NH_3, SO_2, HCl, HONO and HNO_3) at hourly resolution.[62] This effort
133 builds upon our earlier effort[36] to look at the influence of on-road traffic on ambient NH_3
134 variability with different meteorology at the PD site. Details of the MARGA instrument
135 and its performance can be found elsewhere.[36] To complement the information obtained
136 from the MARGA monitoring campaign, additional measurements of tailpipe-emitted
137 NH_3 from 19 different vehicles equipped with three-way catalytic converters were carried
138 out in Nanjing, a megacity in the western Yangtze River Delta region, during April 2016,
139 following a method described elsewhere[63] and briefly summarized in SI Text S1.

140 **2.3 Laboratory analysis**

141 NH_4^+ concentrations in the H_2SO_4 absorbing solutions were measured using a
142 Dionex™ ICS-5000$^+$ system (Thermo Fisher Scientific, Sunnyvale, USA) at the clean
143 laboratory (class 1000) of Yale-NUIST Center on Atmospheric Environment. The IC
144 system was equipped with an automated sampler (AS-DV). NH_4^+ in solutions was
145 measured using an IonPac CG12A guard column and CS12A separation column with
146 an aqueous methanesulfonic acid (MSA, 30 mM L^{-1}) eluent at a flow rate of 1 mL min^{-1}.

147 For the Ogawa passive samples, each filter pad was soaked in 8 mL deionized water
148 (18 MΩ·cm) in a 15 mL vial for 30 min with occasional shaking. Concentrations of NH_4^+
149 in extracts were analyzed using an ion chromatography system (883 Basic IC plus,
150 Metrohm Co., Switzerland) equipped with a Metrosep C4/4.0 cation column. The eluent
151 was 1.0 mmol L^{-1} HNO_3 + 1.0 mmol L^{-1} 2,6-pyridine dicarboxylic acid. The detection limit
152 for NH_4^+ was 2.8 μg L^{-1}, corresponding to an ambient NH_3 concentration of 0.1 ppb for a
153 seven-day sample.

154 For isotopic analysis, a robust and quantitative chemical method was used to
155 determine δ^{15}N-NH_4^+ based on the isotopic analysis of nitrous oxide (N_2O),[64] as detailed
156 and successfully applied in our previous studies.[61, 65] One of the advantages of this
157 method is that it is more suitable for low volume samples including those with low
158 nitrogen concentration. The standard deviation of δ^{15}N measurements determined from
159 the replicates is less than 0.3‰.

160 **2.4 Ammonia modeling**

The Community Multiscale Air Quality (CMAQ, v5.0.1) chemical transport model was used to simulate hourly NH_3 and NH_4^+ concentrations in Shanghai with a 12 × 12 km^2 grid resolution.[66] Meteorological inputs were generated with the Weather Research and Forecasting (WRF v3.6.1) model and the National Centers for Environmental Prediction FNL Operational Model Global Tropospheric Analyses. The tropospheric analyses dataset was used to provide initial and boundary conditions. A multi-resolution emission inventory for China developed by Tsinghua University (http://www.meicmodel.org) was used to define monthly anthropogenic emissions from China. Anthropogenic emissions in 2012 including NH_3, SO_2, NO_x, volatile organic compounds, and PM were re-gridded to the model grids. Open biomass burning emissions were generated from the Fire INventory from NCAR, which is based on satellite observations.[66] Dust and sea salt emissions were generated online during the CMAQ simulations. Biogenic emissions were generated using the Model for Emissions of Gases and Aerosols from Nature (v2.1). [66] The model configurations of CMAQ and WRF are similar to those utilized in a previous nationwide study.[66]

2.5 Bayesian mixing model

Isotopic mixing models allow us to estimate the proportional contributions of multiple sources (emission sources of NH_3 in this study) within a mixture (the ambient NH_3 in this study).[67] By explicitly reflecting the uncertainties associated with multiple sources, isotope fractionation, and isotopic signatures, the application of Bayesian methods to stable isotope mixing models is able to generate robust probability estimates of source proportions, being more appropriate in natural systems than simple linear mixing models.[68, 69] Here a novel Bayesian methodology for analyzing mixing models implemented in the software package SIAR (Stable Isotope Analysis in R)[70] was used to resolve multiple NH_3 source categories by generating potential solutions of source apportionment as true probability distributions. The generation of such source contribution probability distributions is helpful in estimating likely ranges of source contributions when the system solution is under-constrained (i.e., the number of sources exceeds the number of different isotope system tracers + 1). The SIAR package is available to download from the packages section of the Comprehensive R Archive

Network site (CRAN) - http://cran.r-project.org/, and has been widely applied in a number of fields.[71-75] Model frame and computing methods are detailed in SI Text S2.

A comprehensive pool of isotopic source signatures of NH_3 (IS_NH_3) has been established in our previous work[65] with the exception of "NH_3 slip from coal-fired power plant".[76] These IS_NH_3 are typically found to lie between -50‰ and -10‰, with occasional overlap between signatures from different source types.[65, 77] The NH_3 emissions were defined by four distinct source categories (Table 1): livestock breeding (-29.1 ± 1.7‰), N-fertilizer application (-50.0 ± 1.8‰; urea application), combustion-related sources (-14.0 ± 2.7‰; on-road traffic, NH_3 slip from coal-fired power plants), and urban waste volatilized sources (-37.8 ± 3.6‰; wastewater treatment, municipal solid waste, and human excreta).

2.6 Ancillary information

Hourly meteorological parameters (MSO Weather Sensor, MetOne Instruments, USA; including wind direction, wind speed, relative humidity or RH, and temperature or *T*) in Shanghai were provided by the Shanghai Meteorological Bureau. Bivariate polar plots

206 (BPP) were used to demonstrate how NH_3 concentrations vary with wind direction and
207 wind speed in polar coordinates, an effective diagnostic technique for discriminating
208 different source regions.[78-81] For creating BBPs, the open-source software "openair" in
209 R was used.[79]

210 ## 3 Results and discussion

211 ### 3.1 Spatially-revolved sampling reveals urban areas as a hot spot of atmospheric NH_3

212 A total of 702 duplicate passive samples were collected in this study. The passive
213 sampling sites are divided into three types: urban (461 samples), suburban (108
214 samples), and rural (133 samples), based on local land use and economic activities.
215 Weekly variations of atmospheric NH_3 concentrations at each observation site, and
216 annual and seasonal average NH_3 concentrations (mean ± 1 σ) among different sites
217 and site categories are plotted in Fig. 2 and Fig. 3, respectively. The observations from
218 the Ogawa passive samplers are mainly used to illustrate spatial distributions rather
219 than temporal variations of NH_3, due to their relatively coarse time resolution.

220 Taking the results of all weekly samples as a whole, atmospheric NH_3 concentrations
221 in Shanghai range from 1.2 to 23.1 ppb, with a mean (± 1σ) and median value of 7.3 (±
222 3.1) and 6.8 ppb, respectively. Domestically, the annual average NH_3 concentrations in
223 northern China (e.g., Beijing (23.5 ± 18.0 ppb)[82] and Xi'an (18.6 ppb on average)[83]) are
224 much higher than our observations in Shanghai (Table 2). This can be partly explained
225 by a higher soil pH in the North China Plain and the Guanzhong Plain where Beijing and
226 Xi'an are located, respectively,[84] which promotes loss of NH_3.[85] Instead, the Yangtze
227 River Delta region (including Shanghai) is dominated by acid soils of paddy fields.[86]
228 Internationally, the average NH_3 level we measured in Shanghai is generally similar to
229 observations in developed cities like Seoul in S. Korea[87] and Houston in the U.S.,[88] but
230 much lower than in some cities in developing countries. This is particularly true when
231 comparing with cities in South Asia (e.g., Delhi in India;[89] Table 2), where there is a lack
232 of basic sanitation facilities (e.g., public flush toilets), and significant animal populations
233 (such as cows) coexist with people in urban areas.[90] The high NH_3 concentrations
234 measured at surface sites in South Asia are consistent with the spatial patterns
235 determined from recent satellite remote sensing observations.[91, 92] It is worth noting that

from measurements in the Shanghai Jinshan chemical industry park (Fig. 2), Wang et al.[93] showed a much higher NH_3 concentration (17.6 ± 9.5 ppb) with abrupt concentration changes on an hourly basis, a result of the strong influence of variable industrial emissions in the vicinity.

NH_3 levels were found to exhibit modest gradients across the study region, with mean NH_3 concentrations ranging from 4.8 (CM rural site) to 9.7 ppb (HP urban site) (Fig. 2 and Fig. 3c). As discussed above, on a regional scale, NH_3 is mainly emitted from animal housing, manure storage, and land-spread manure, and to a smaller extent from mineral fertilizer application. The emission strengths of these sources are primarily determined by the activity of microbes, which is highly dependent on temperature.[94] Hence, rural areas with strong agricultural sources, are expected to experience increased emissions in summertime. Indeed, in our study, the average NH_3 concentrations in summer are higher than in other seasons for each land use category (Fig. 3b) and site (Fig. 3d), signifying the importance of volatilized NH_3 sources in the region (see discussion later). Somewhat surprisingly, however, the lowest average

ambient NH_3 concentrations are found at rural sites such as CM (4.8 ± 2.6 ppb) and SY (6.3 ± 4.1 ppb), which are in active agricultural areas (Fig. 3c). Although the average NH_3 concentration at the rural DH site (7.4 ± 4.1 ppb) is higher than 7 of the other 13 sites (Fig. 3c), the overall average NH_3 concentration observed at urban sites (7.8 ± 2.9 ppb) is significantly higher than at suburban (6.8 ± 3.1 ppb, $p < 0.01$) and rural (6.2 ± 3.8 ppb, $p < 0.01$) sites (Fig. 3a). In fact, urban enrichment of NH_3 in Shanghai is not unique. In Table 2 we compile previous studies in which urban NH_3 concentrations are comparable with or higher than suburban and rural NH_3 concentrations. In brief, our results demonstrate that urban areas, without agricultural activities, can also be an important source of NH_3 emissions.

Temperature is the key driver of NH_3 emissions from volatility-driven sources; observations of NH_3 volatilization by Sommer et al.[98] found that NH_3 emissions after 6 h of surface applied cattle slurry were exponentially related to temperature ($r^2 > 0.80$). As shown in Fig. 2 and Fig. 3d, the average NH_3 concentrations are higher in summer and lower in winter. This is particularly true at rural sites, consistent with dominant,

266 temperature-sensitive emission of NH_3 from agricultural sources like livestock waste and
267 fertilizer application. There are also other temperature-sensitive sources in urban areas
268 like wastewater, household garbage, golf turf, and human excreta; the latter two are
269 often overlooked but important NH_3 sources in urban China.[44, 99] Although still
270 recognized as a luxury sport by most Chinese people, golf is increasingly popular.[44] In
271 contrast to Western industrialized countries, golf courses in China tend to operate in
272 urban areas, which are closer to the affluent consumer.[44] Also different from other
273 developed countries, human excreta in urban China is typically first stored in a three-
274 grille septic tank beneath the building.[61] After a series of anaerobic decomposition
275 processes, a substantial amount of odors (including NH_3) will be generated and emitted
276 through a ceiling duct.[61]

277 From a climate perspective, differences in temperature and other meteorological
278 parameters (e.g., precipitation, wind speed, planetary boundary layer) over the
279 Shanghai region are minor.[36] Interestingly, the lowest NH_3 concentrations at urban
280 Shanghai sites were not observed in the winter, while the NH_3 difference between

summer and winter is much lower at urban sites than at rural sites in our dataset (Fig. 3). These observations suggest that there may be some other temperature-independent NH_3 sources present in urban areas.

3.2 Significant influences of non-agricultural NH_3 emissions in the urban atmosphere

The analysis of weekly NH_3 samples collected from our network of sites spanning various land use categories indicates that the enhancement of atmospheric NH_3 at urban sites reflects a mix of agricultural and non-agricultural NH_3 emissions. To further explore and compare the influences of various NH_3 sources on ambient NH_3 in urban and rural atmospheres, we can examine the year-round, hourly observations of NH_3 at the urban PD and rural DH sites (Fig. 1). By combining hourly concentration, wind speed, and wind direction measurements, bivariate polar plots (BPP) can be constructed to identify source regions of near-ground pollutants like NH_3, an approach that has proven to be a more suitable tool than back trajectory-based methods.[78, 80, 81]

As illustrated in Fig. 4a, there are large temporal variations in NH_3 concentrations at the urban PD and rural DH site, with their hourly NH_3 concentrations ranging from 0.1 to 36.4 μg m^{-3} (mean ± 1σ = 5.9 ± 4.5 μg m^{-3}; median = 4.8 μg m^{-3}; n = 7897; 90.1% data

297 availability) and 0.1 to 33.0 μg m^{-3} (mean ± 1σ = 6.6 ± 4.1 μg m^{-3}; median = 5.9 μg m^{-3};
298 n = 8204; 93.7% data availability), respectively. The NH_3 concentration spikes at both
299 sites are concentrated in summer (June, July, and August), and their smoothed trends
300 are generally consistent with the variation of temperature. These findings suggest that
301 volatilized NH_3 emissions are a regionally important NH_3 source in Shanghai.
302 Also included in Fig. 4 are, to help further identify specific sources, the diurnal profiles
303 of NH_3 and temperature at DH and PD. At the rural DH site, diurnal variations of NH_3
304 concentrations are highly correlated with temperature (r^2 = 0.98, p < 0.01; Fig. 4b),
305 indicating the predominant role of volatilization-related NH_3 sources in rural areas. In
306 eastern China (including Shanghai), agricultural sources (livestock feeding and N-
307 fertilizer application) make up nearly 90% of the total NH_3 emissions.[22] Indeed, in Fig.
308 5a, the BPP analysis shows that high NH_3 concentrations at DH are associated with air
309 flows from the southwest and the southeast but infrequently from the northwest. This
310 can be explained by the large lake Dianshanhu in the northwest, which has negligible
311 NH_3 emission potential.[44, 45] The south and east side of the lake is covered by intensive
312 cultivation areas, with modern agriculture facilities.[61] The areas to the southeast of the

313 sampling site have been described as the "backyard garden" of Shanghai, renowned for
314 its idyllic scene, and are a regional hot spot of agricultural NH_3 emissions.[22, 61]
315 At the urban PD site, however, distinctly different pictures of the diurnal profiles of NH_3
316 and temperature are observed (see Fig. 4c and 4d), suggesting a complex mix of NH_3
317 source contributions. Specifically, there is no correlation between NH_3 concentration
318 and temperature on a diurnal basis (Fig. 4d). The average concentrations of NH_3 show
319 a well-marked bimodal pattern, which is generally similar to the diurnal evolution of
320 urban traffic flow in Shanghai.[17] Previous observations have also shown coincident
321 enhancements of NH_3 and carbon monoxide (CO) in the Shanghai urban atmosphere.[36]
322 Following a stable period of NH_3 concentrations between 22:00 and 5:00 (5.7 ± 0.1 μg
323 m^{-3}), the maximum NH_3 concentration occurs in the morning rush hour (7.0 μg m^{-3},
324 10:00), 22% higher than the overnight level. In Fig. 5b, the Shanghai metropolitan area
325 to the southwest and the suburban Pudong District to the southeast are indicated as two
326 prominent NH_3 source regions. The metropolitan area is densely populated with intense
327 traffic, representing an important source region of non-agricultural NH_3 emissions
328 (including vehicles). The suburban Pudong District, for long stretches, serves as the

329 primary animal feeding operation region in Eastern China, where almost all livestock
330 farms are focused on hog rearing.[61]

331 To further examine the NH_3 emissions potential from vehicles, we measured NH_3
332 concentrations emitted from tailpipe exhaust of 19 different vehicles equipped with
333 TWCs. The average NH_3 concentration of the total 57 samples (10.2 ppm) is four orders
334 of magnitude higher than the ambient NH_3 concentrations. Considering the huge
335 automobile inventory in Shanghai (nearly 3.3 million in 2015),[36] our study strongly
336 suggests that on-road traffic is an important NH_3 source in the urban atmosphere.

337 **3.3 NH_3 from non-agricultural rival agricultural emissions in the urban atmosphere**

338 Figure 6 compares model simulations and measurements of hourly NH_3 concentration
339 at the rural DH and urban PD sites. The average measured and predicted NH_3
340 concentrations at DH are similar, although the variability in the model predictions is
341 much larger than the observations, perhaps reflecting the coarse time resolution of the
342 emission inventory used. It is noteworthy that the average NH_3 concentration at the rural
343 DH site is accurate without any non-agricultural NH_3 emissions being included in the

344 model, consistent with our conclusion above that agricultural activities are the
345 predominant NH_3 source in rural areas. At the urban PD site, the simulation with only
346 agricultural NH_3 emissions yields an average predicted NH_3 concentration (3.6 μg m^{-3})
347 that is 47% lower than the average measured concentration (6.7 μg m^{-3}), suggesting
348 that (non-simulated) emissions from non-agricultural activities are important contributors
349 to urban NH_3. Although other factors could contribute to under-prediction of urban NH_3
350 (e.g., incorrectly modeled transport from rural agricultural sources or overestimation of
351 the rate of dry deposition of NH_3 emitted by agricultural sources), past studies suggest
352 that ambient NH_3 concentrations most strongly depend on NH_3 emissions rather than
353 atmospheric processes,[100, 101] suggesting that ignoring non-agricultural NH_3 emissions
354 is likely one of the most important reasons for the low concentration model bias at PD.
355 A quantitative and accurate assessment of NH_3 sources in the urban atmosphere is
356 difficult to obtain solely using the approach described above. Below we demonstrate the
357 complementary use of N isotopes to better constrain NH_3 source contributions at the PD
358 site. Although there is generally not a compelling need to differentiate agricultural vs.
359 non-agricultural emissions contributions in rural areas, the relative contributions of N-

360 fertilizer application and livestock feeding are certainly of interest and isotopic
361 signatures are also used to constrain these source contributions at the rural DH site.

362 Isotope-based source apportionment of atmospheric NH_3 requires a well-established
363 pool of NH_3 isotopic source signatures ($\delta^{15}N$-NH_3) to allow a separation of different
364 sources. From a total of 44 NH_3 source samples in our previous study,[65] we have
365 established a pool of isotopic signatures for the major NH_3 emission sources in Eastern
366 China (Table 1). The NH_3 concentrations and $\delta^{15}N$ values of these samples ranged from
367 33 to 6211 μg m^{-3} and -52.0 to -9.6‰, respectively. Recently, NH_3 slip from coal-fired
368 power plants equipped with selective catalytic reduction (SCR) technology was reported
369 as an important source of NH_3; thus, its isotopic signature, as reported by Felix et al.[76],
370 is also considered in this study. Table 1 shows that these NH_3 sources can be clearly
371 classified into four categories by specific isotope signatures: NH_3 emitted from
372 combustion-related sources has relatively high $\delta^{15}N$ values, allowing them to be
373 distinguished from NH_3 emitted from volatilization processes. The $\delta^{15}N$ values (mean ±
374 1σ) of the Shanghai urban PD site environmental samples collected in July and August

375 of 2015 were -31.72 ± 3.36‰ (ranging from -36.01‰ to -25.40‰, n = 10), close to the
376 δ^{15}N-NH_3 values observed in Beijing (-34.0‰ to -27.2‰, n = 4; a period without strict air
377 quality control measures)[65] and higher than at the rural DH site (-41.03‰, -36.53‰),
378 suggesting a stronger influence of combustion-related sources in the urban atmosphere.

379 At the rural DH site, our earlier analysis demonstrated that rural NH_3 concentrations
380 can be solely attributed to agricultural NH_3 emissions, i.e., livestock breeding (LB) and
381 fertilizer application (FA). Therefore, the isotopic signatures of two sources, i.e., LB and
382 FA, are used as input into the SIAR Bayesian mixing model. The results suggest that on
383 average, LB and FA contribute 51.9% and 48.1% to the measured NH_3 concentrations,
384 respectively (not shown). From the perspective of the emissions inventory, the NH_3
385 emissions from LB and FA contribute 48% and 40% to the total in Eastern China,
386 respectively,[22] in general agreement with our results.

387 At the PD urban site with its more complex NH_3 sources, normal distributions and
388 variation ranges (within 5 and 95 percentiles) of the relative contribution fractions of
389 each source to the ambient NH_3 concentrations were estimated and are depicted in Fig.

7. As a reminder, the availability of only a single isotopic tracer vs. four hypothesized source types, means that there is no unique solution for the system;[102, 103] however, we can identify all possible sets of source contributions that reproduce the observed isotopic signature. The utility of this analysis will depend, to a large extent, on how narrow the source contribution ranges are for each source. In our analysis, fossil fuel-related sources (FF) and fertilizer application (FA) have relatively low variation ranges (Fig. 7), indicating that they are better constrained than livestock breeding (LB; -31.7% to -27.1%) and urban waste volatilized (UW; -41.9% to -29.9%) sources. This is because the isotopic signatures of LB and UW are distributed in the middle of the source pool, where their contributions to the $\delta^{15}N$ values of the ambient NH_3 (-36.01‰ to -25.40‰) are less well constrained. The pie chart in Fig. 7 illustrates the overall mean contribution proportions.. While estimates of the mean values are inherently uncertain,[102] the four source contribution distribution estimates strongly suggest that all four source types make substantial contributions to the NH_3 concentrations measured at the urban PD site. Further, this isotopic analysis lends further confidence to our earlier conclusion from the WRF-CMAQ model vs. observations comparison that non-

406 agricultural sources rival agricultural sources in terms of contributing to ambient NH_3 in
407 the urban atmosphere.

408 Fossil fuel-related sources are identified as an important contributor to ambient NH_3
409 concentrations at PD. Although NH_3 emissions from coal and biomass burning are
410 observed,[26, 30] they are not comparable with the magnitude of vehicular NH_3 emissions
411 and NH_3 slip from SCR-equipped coal-fired power plant (CFPP).[30, 37] Recently, a five-
412 year plan was introduced in China to slash coal consumption from CFPP and household
413 sectors.[77] For example, in 2016, all CFPPs in Beijing were replaced with gas-fired
414 power plants to cut pollution.[77] The replacement by the four gas-fired power plants will
415 help cut emissions by 10000 tons of SO_2 and 19000 tons of NO annually.[77] Although
416 NH_3 slip is a common issue with SCR technology used in CFPP for the removal of NO,
417 the mass concentration of NH_3 (typically 3-5 mg NH_3 m^{-3}) in flue gases is two or three
418 orders of magnitude smaller than that of NO_x.[77] Therefore, we suspect that the share of
419 NH_3 emissions from SCR-equipped CFPP in urban areas is relatively small and will
420 decrease continuously in China. In the US, it is estimated that 5% of the national NH_3

emissions are derived from motor vehicles, while this figure is estimated at 12% for the UK, with almost all the remaining NH_3 coming from agricultural processes.[45] In China, all new light-duty vehicles were required to install TWC since 2009.[44] In Table S1, we have provided direct evidence that TWC-equiped vehicles are an important urban source of NH_3. Thus expanding vehicular NH_3 emissions in urban China can be expected. Indeed, the average contribution of fossil fuel-related sources derived from the Bayesian isotopic mixing model (28.6%) is close to the share of on-road traffic (22.3%) we estimated above based on NH_3 concentration analysis at PD. This suggests that fossil fuel-derived NH_3 concentrations in urban Shanghai are primarily emitted from on-road traffic.

4 Implications and outlook

The present study outlines a framework to integrate NH_3 concentration measurements, atmospheric transport modeling, and isotope-based source apportionment to address a long-standing and ongoing controversy regarding sources of NH_3 in the urban atmosphere. We validate the feasibility of this approach by

436 application to the Yangtze River Delta region, with a focus on the megacity of Shanghai.
437 Results from a Shanghai passive NH_3 monitoring network (14 locations) reveal a
438 broadly homogeneous distribution of NH_3 concentrations throughout the region and
439 pinpoint urban areas as a hot spot of NH_3. The acquired data also provide a baseline
440 toward tracking future NH_3 emissions changes. The year-round online measurements of
441 NH_3 at an urban and rural site, and a comparison against concentrations simulated by
442 the WRF-CMAQ chemical transport model, demonstrate that NH_3 in the rural
443 atmosphere can be attributed to emissions from agricultural sources, while there is a
444 significant contribution from non-agricultural NH_3 emissions, particularly vehicular NH_3
445 emissions, in the urban atmosphere. Isotope-based source apportionment of NH_3 in the
446 urban atmosphere further indicates that non-agricultural NH_3 emissions, missing from
447 the current emission inventory, could well rival agricultural NH_3 emissions in terms of
448 contributing to ambient NH_3.

449 Given the central role of NH_3 in the formation of secondary inorganic aerosols and
450 resulting haze, our results are of critical importance for China as it seeks to curb its

severe $PM_{2.5}$ pollution. Additional useful investigative steps could include: (1) sensitivity analyses with the WRF-CMAQ model to further diagnose the importance of non-agricultural NH_3 emissions through developing a gridded non-agricultural NH_3 emissions inventory with high time resolution; (2) collecting NH_3 and aerosol NH_4^+ for simultaneously determining the mass concentrations and isotopic compositions at high time resolution; and (3) improving the pool of isotopic source signatures of NH_3 from fuel-related sources.

ASSOCIATED CONTENT

Supporting Information.

The following files are available free of charge (PDF). Figure S1. A summary of the average monthly temperature and precipitation in Shanghai. Text S1. Details regarding the method used to collect vehicle-emitted NH_3. Text S2. Model frame and computing methods of the SIAR (Stable Isotope Analysis in R).

AUTHOR INFORMATION

Corresponding Author

*Corresponding authors: Yanlin Zhang (dryanlinzhang@outlook.com), Congrui Deng (congruideng@fudan.edu.cn).

Notes

The authors declare that they have no conflict of interest.

ACKNOWLEDGMENT

This study was supported by the National Key R&D Program of China (Grant no. 2017YFC0210101), National Natural Science Foundation of China (Grant nos. 41705100, 91644103), the Provincial Natural Science Foundation of Jiangsu (Grant nos. BK20180040, BK20170946), and University Science Research Project of Jiangsu Province (17KJB170011). A tip of the hat to two ladies, Yan Zhang and Meigui Wang, who pulled all of their weight at home so that Yunhua Chang could concentrate on data analysis and paper writing.

REFERENCES

1. Wang, Y.; Zhang, Q. Q.; He, K.; Zhang, Q.; Chai, L., Sulfate-nitrate-ammonium aerosols over China: Response to 2000-2015 emission changes of sulfur dioxide, nitrogen oxides, and ammonia. *Atmos. Chem. Phys.* **2013,** *13*, (5), 2635-2652.
2. Walker, J. M.; Philip, S.; Martin, R. V.; Seinfeld, J. H., Simulation of nitrate, sulfate, and ammonium aerosols over the United States. *Atmos. Chem. Phys.* **2012,** *12*, (22), 11213-11227.
3. Zhang, X. Y.; Wang, Y. Q.; Niu, T.; Zhang, X. C.; Gong, S. L.; Zhang, Y. M.; Sun, J. Y., Atmospheric aerosol compositions in China: Spatial/temporal variability, chemical signature, regional haze distribution and comparisons with global aerosols. *Atmos. Chem. Phys.* **2012,** *12*, (2), 779-799.
4. Yang, F.; Tan, J.; Zhao, Q.; Du, Z.; He, K.; Ma, Y.; Duan, F.; Chen, G.; Zhao, Q., Characteristics of $PM_{2.5}$ speciation in representative megacities and across China. *Atmos. Chem. Phys.* **2011,** *11*, (11), 5207-5219.
5. Huang, R. J.; Zhang, Y.; Bozzetti, C.; Ho, K. F.; Cao, J. J.; Han, Y.; Daellenbach, K. R.; Slowik, J. G.; Platt, S. M.; Canonaco, F.; Zotter, P.; Wolf, R.; Pieber, S. M.; Bruns, E. A.; Crippa, M.; Ciarelli, G.; Piazzalunga, A.; Schwikowski, M.; Abbaszade, G.; Schnelle-Kreis, J.; Zimmermann, R.; An, Z.; Szidat, S.; Baltensperger, U.; El Haddad, I.; Prevot, A. S., High secondary aerosol contribution to particulate pollution during haze events in China. *Nature* **2014,** *514*, (7521), 218-222.
6. Paulot, F.; Jacob, D. J., Hidden cost of US agricultural exports: Particulate matter from ammonia emissions. *Environ. Sci. Technol.* **2014,** *48*, (2), 903-908.
7. Pinder, R. W.; Adams, P. J.; Pandis, S. N., Ammonia emission controls as a cost-effective strategy for reducing atmospheric particulate matter in the eastern United States. *Environ. Sci. Technol.* **2007,** *41*, (2), 380-386.
8. Heo, J.; Adams, P. J.; Gao, H. O., Public health costs of primary $PM_{2.5}$ and inorganic $PM_{2.5}$ precursor emissions in the United States. *Environ. Sci. Technol.* **2016,** *50*, (11), 6061-6070.
9. Brunekreef, B.; Harrison, R. M.; Künzli, N.; Querol, X.; Sutton, M. A.; Heederik, D. J. J.; Sigsgaard, T., Reducing the health effect of particles from agriculture. *Lancet Respiratory Medicine* **2015,** *3*, (11), 831-832.
10. Lee, C. J.; Martin, R. V.; Henze, D. K.; Brauer, M.; Cohen, A.; Donkelaar, A. V., Response of global particulate-matter-related mortality to changes in local precursor emissions. *Environ. Sci. Technol.* **2015,** *49*, (7), 4335-4344.
11. Warner, J. X.; Dickerson, R. R.; Wei, Z.; Strow, L. L.; Wang, Y.; Liang, Q., Increased atmospheric ammonia over the world's major agricultural areas detected from space. *Geophys. Res. Lett.* **2017,** *44*, (6), 2875-2884.
12. Liu, L.; Zhang, X.; Xu, W.; Liu, X.; Li, Y.; Lu, X.; Zhang, Y.; Zhang, W., Temporal characteristics of atmospheric ammonia and nitrogen dioxide over China based on emission data, satellite observations and atmospheric transport modeling since 1980. *Atmos. Chem. Phys.* **2017,** *17*, (15), 9365-9378.
13. Kang, Y.; Liu, M.; Song, Y.; Huang, X.; Yao, H.; Cai, X.; Zhang, H.; Kang, L.; Liu, X.; Yan, X.; He, H.; Zhang, Q.; Shao, M.; Zhu, T., High-resolution ammonia emissions inventories in China from 1980 to 2012. *Atmos. Chem. Phys.* **2016,** *16*, (4), 2043-2058.
14. Aneja, V. P.; Schlesinger, W. H.; Erisman, J. W., Farming pollution. *Nat. Geosci.* **2008,** *1*, (7), 409-411.
15. Reis, S.; Pinder, R.; Zhang, M.; Lijie, G.; Sutton, M., Reactive nitrogen in atmospheric emission inventories. *Atmos. Chem. Phys.* **2009,** *9*, (19), 7657-7677.
16. Van Damme, M.; Wichink Kruit, R. J.; Schaap, M.; Clarisse, L.; Clerbaux, C.; Coheur, P.; Dammers, E.; Dolman, A. J.; Erisman, J. W., Evaluating 4 years of atmospheric ammonia (NH_3) over Europe using IASI satellite observations and LOTOS-EUROS model results. *J. Geophys. Res.* **2014,** *119*, (15), 9549-9566.
17. Xu, P.; Liao, Y. J.; Lin, Y. H.; Zhao, C. X.; Yan, C. H.; Cao, M. N.; Wang, G. S.; Luan, S. J., High-resolution inventory of ammonia emissions from agricultural fertilizer in China from 1978 to 2008. *Atmos. Chem. Phys.* **2016,** *16*, (3), 1207-1218.
18. Bouwman, A. F.; Lee, D. S.; Asman, W. A. H.; Dentener, F. J.; Van Der Hoek, K. W.; Olivier, J. G. J., A global high-resolution emission inventory for ammonia. *Global Biogeochem. Cy.* **1997,** *11*, (4), 561-587.
19. Heald, C. L.; Collett Jr, J.; Lee, T.; Benedict, K.; Schwandner, F.; Li, Y.; Clarisse, L.; Hurtmans, D.; Van Damme, M.; Clerbaux, C., Atmospheric ammonia and particulate inorganic nitrogen over the United States. *Atmos. Chem. Phys.* **2012,** *12*, (21), 10295-10312.
20. Zhang, L.; Chen, Y.; Zhao, Y.; Henze, D. K.; Zhu, L.; Song, Y.; Paulot, F.; Liu, X.; Pan, Y.; Lin, Y.; Huang, B., Agricultural ammonia emissions in China: Reconciling bottom-up and top-down estimates. *Atmos. Chem. Phys.* **2018,** *18*, (1), 339-355.

21. Balasubramanian, S.; Koloutsou-Vakakis, S.; McFarland, D. M.; Rood, M. J., Reconsidering emissions of ammonia from chemical fertilizer usage in Midwest USA. *J. Geophys. Res.* **2015,** *120*, (12), 6232-6246.
22. Huang, C.; Chen, C. H.; Li, L.; Cheng, Z.; Wang, H. L.; Huang, H. Y.; Streets, D. G.; Wang, Y. J.; Zhang, G. F.; Chen, Y. R., Emission inventory of anthropogenic air pollutants and VOC species in the Yangtze River Delta region, China. *Atmos. Chem. Phys.* **2011,** *11*, (9), 4105-4120.
23. Aneja, V. P.; Schlesinger, W. H.; Erisman, J. W., Effects of agriculture upon the air quality and climate: Research, policy, and regulations. *Environ. Sci. Technol.* **2009,** *43*, (12), 4234-4240.
24. Wang, S.; Xing, J.; Jang, C.; Zhu, Y.; Fu, J. S.; Hao, J., Impact assessment of ammonia emissions on inorganic aerosols in East China using response surface modeling technique. *Environ. Sci. Technol.* **2011,** *45*, (21), 9293-300.
25. Zhang, C.; Geng, X.; Wang, H.; Zhou, L.; Wang, B., Emission factor for atmospheric ammonia from a typical municipal wastewater treatment plant in South China. *Environ. Pollut.* **2017,** *220*, 963-970.
26. Li, Q.; Jiang, J.; Cai, S.; Zhou, W.; Wang, S.; Duan, L.; Hao, J., Gaseous ammonia emissions from coal and biomass combustion in household stoves with different combustion efficiencies. *Environ. Sci. Technol. Lett.* **2016,** *3*, (3), 98-103.
27. Reche, C.; Viana, M.; Pandolfi, M.; Alastuey, A.; Moreno, T.; Amato, F.; Ripoll, A.; Querol, X., Urban NH_3 levels and sources in a Mediterranean environment. *Atmos. Environ.* **2012,** *57*, 153-164.
28. Suarez-Bertoa, R.; Zardini, A.; Astorga, C., Ammonia exhaust emissions from spark ignition vehicles over the new European driving cycle. *Atmos. Environ.* **2014,** *97*, 43-53.
29. Teng, X.; Hu, Q.; Zhang, L.; Qi, J.; Shi, J.; Xie, H.; Gao, H.; Yao, X., Identification of major sources of atmospheric NH_3 in an urban environment in Northern China during wintertime. *Environ. Sci. Technol.* **2017,** *51*, (12), 6839-6848.
30. Meng, W.; Zhong, Q.; Yun, X.; Zhu, X.; Huang, T.; Shen, H.; Chen, Y.; Chen, H.; Zhou, F.; Liu, J.; Wang, X.; Zeng, E. Y.; Tao, S., Improvement of a global high-resolution ammonia emission inventory for combustion and industrial sources with new data from the residential and transportation sectors. *Environ. Sci. Technol.*, **2017**, *51* (5), 2821-2829.
31. Pierson, W. R.; Brachaczek, W. W., Emissions of ammonia and amines from vehicles on the road. *Environ. Sci. Technol.* **1983,** *17*, (12), 757-760.
32. Heeb, N. V.; Forss, A. M.; Brühlmann, S.; Lüscher, R.; Saxer, C. J.; Hug, P., Three-way catalyst-induced formation of ammonia—velocity-and acceleration-dependent emission factors. *Atmos. Environ.* **2006,** *40*, (31), 5986-5997.
33. Fenn, M. E.; Bytnerowicz, A.; Schilling, S. L.; Vallano, D. M.; Zavaleta, E. S.; Weiss, S. B.; Morozumi, C.; Geiser, L. H.; Hanks, K., On-road emissions of ammonia: an underappreciated source of atmospheric nitrogen deposition. *Sci. Total Environ.* **2018,** *625*, 909-919.
34. Kean, A. J.; Harley, R. A.; Littlejohn, D.; Kendall, G. R., On-road measurement of ammonia and other motor vehicle exhaust emissions. *Environ. Sci. Technol.* **2000,** *34*, (17), 3535-3539.
35. Zhang, Y.; Tang, A.; Wang, D.; Wang, Q.; Benedict, K.; Zhang, L.; Liu, D.; Li, Y.; Collett Jr., J. L.; Sun, Y.; Liu, X., The vertical variability of ammonia in urban Beijing, China. *Atmos. Chem. Phys.* **2018,** *18*, 16385-16398.
36. Chang, Y.; Zou, Z.; Deng, C.; Huang, K.; Collett, J. L.; Lin, J.; Zhuang, G., The importance of vehicle emissions as a source of atmospheric ammonia in the megacity of Shanghai. *Atmos. Chem. Phys.* **2016,** *16*, (5), 3577-3594.
37. Sun, K.; Tao, L.; Miller, D. J.; Pan, D.; Golston, L. M.; Zondlo, M. A.; Griffin, R. J.; Wallace, H. W.; Leong, Y. J.; Yang, M. M.; Zhang, Y.; Mauzerall, D. L.; Zhu, T., Vehicle emissions as an important urban ammonia source in the United States and China. *Environ. Sci. Technol.* **2017,** *51*, (4), 2472-2481.
38. Fraser, M. P.; Cass, G. R., Detection of excess ammonia emissions from in-use vehicles and the implications for fine particle control. *Environ. Sci. Technol.* **1998,** *32*, (8), 1053-1057.
39. Huai, T.; Durbin, T. D.; Miller, J. W.; Pisano, J. T.; Sauer, C. G.; Rhee, S. H.; Norbeck, J. M., Investigation of NH_3 emissions from new technology vehicles as a function of vehicle operating conditions. *Environ. Sci. Technol.* **2003,** *37*, (21), 4841-4847.
40. Liu, T.; Wang, X.; Wang, B.; Ding, X.; Deng, W.; Lü, S.; Zhang, Y., Emission factor of ammonia (NH_3) from on-road vehicles in China: Tunnel tests in urban Guangzhou. *Environ. Res. Lett.* **2014,** *9*, (6), 064027.

41. Kean, A. J.; Littlejohn, D.; Ban-Weiss, G. A.; Harley, R. A.; Kirchstetter, T. W.; Lunden, M. M., Trends in on-road vehicle emissions of ammonia. *Atmos. Environ.* **2009,** *43*, (8), 1565-1570.
42. Nowak, J. B.; Huey, L. G.; Russell, A. G.; Tian, D.; Neuman, J. A.; Orsini, D.; Sjostedt, S. J.; Sullivan, A. P.; Tanner, D. J.; Weber, R. J.; Nenes, A.; Edgerton, E.; Fehsenfeld, F. C., Analysis of urban gas phase ammonia measurements from the 2002 Atlanta Aerosol Nucleation and Real-Time Characterization Experiment (ANARChE). *J. Geophys. Res.* **2006,** *111*, (D17), https://doi.org/10.1029/2006JD007113.
43. Yao, X.; Hu, Q.; Zhang, L.; Evans, G. J.; Godri, K. J.; Ng, A. C., Is vehicular emission a significant contributor to ammonia in the urban atmosphere? *Atmos. Environ.* **2013,** *80*, 499-506.
44. Chang, Y. H., Non-agricultural ammonia emissions in urban China. *Atmos. Chem. Phys. Discussions* **2014,** *14*, (6), 8495-8531.
45. Sutton, M. A.; Dragosits, U.; Tang, Y.; Fowler, D., Ammonia emissions from non-agricultural sources in the UK. *Atmos. Environ.* **2000,** *34*, (6), 855-869.
46. Battye, W.; Aneja, V. P.; Roelle, P. A., Evaluation and improvement of ammonia emissions inventories. *Atmos. Environ.* **2003,** *37*, (27), 3873-3883.
47. Li, Y.; Thompson, T. M.; Van Damme, M.; Chen, X.; Benedict, K. B.; Shao, Y.; Day, D.; Boris, A.; Sullivan, A. P.; Ham, J.; Whitburn, S.; Clarisse, L.; Coheur, P. F.; Collett Jr, J. L., Temporal and spatial variability of ammonia in urban and agricultural regions of northern Colorado, United States. *Atmos. Chem. Phys.* **2017,** *17*, (10), 6197-6213.
48. Puchalski, M. A.; Sather, M. E.; Walker, J. T.; Lehmann, C. M.; Gay, D. A.; Mathew, J.; Robarge, W. P., Passive ammonia monitoring in the United States: Comparing three different sampling devices. *J. Environ. Monit.* **2011,** *13*, (11), 3156-67.
49. Li, Y.; Schichtel, B. A.; Walker, J. T.; Schwede, D. B.; Chen, X.; Lehmann, C. M. B.; Puchalski, M. A.; Gay, D. A.; Collett, J. L., Increasing importance of deposition of reduced nitrogen in the United States. *Proc. Natl. Acad. Sci. U. S. A.* **2016,** *113*, (21), 5874-5879.
50. Liu, X.; Zhang, Y.; Han, W.; Tang, A.; Shen, J.; Cui, Z.; Vitousek, P.; Erisman, J. W.; Goulding, K.; Christie, P.; Fangmeier, A.; Zhang, F., Enhanced nitrogen deposition over China. *Nature* **2013,** *494*, 459-463.
51. Lu, C.; Tian, H., Half-century nitrogen deposition increase across China: a gridded time-series data set for regional environmental assessments. *Atmos. Environ.* **2014,** *97*, 68-74.
52. Lü, C.; Tian, H., Spatial and temporal patterns of nitrogen deposition in China: Synthesis of observational data. *J. Geophys. Res.* **2007,** *112*, (D22), https://doi.org/10.1029/2006JD007990.
53. Jia, Y.; Yu, G.; He, N.; Zhan, X.; Fang, H.; Sheng, W.; Zuo, Y.; Zhang, D.; Wang, Q., Spatial and decadal variations in inorganic nitrogen wet deposition in China induced by human activity. *Sci. Rep.*, **2014,** *4*, 3763.
54. Liu, J.; Kuang, W.; Zhang, Z.; Xu, X.; Qing, Y.; Ning, J.; Zhou, W.; Zhang, S.; Li, R., Spatiotemporal characteristics, patterns, and causes of land-use changes in China since the late 1980s. *J. Geogr. Sci.* **2014,** *24*, (2), 195-210.
55. Ma, T.; Zhou, C.; Pei, T.; Haynie, S.; Fan, J., Quantitative estimation of urbanization dynamics using time series of DMSP/OLS nighttime light data: a comparative case study from China's cities. *Remote Sens. Environ.* **2012,** *124*, 99-107.
56. Guan, X.; Wei, H.; Lu, S.; Dai, Q.; Su, H., Assessment on the urbanization strategy in China: Achievements, challenges and reflections. *Habitat Int.* **2018,** *71*, 97-109.
57. Haas, J.; Ban, Y., Urban growth and environmental impacts in Jing-Jin-Ji, the Yangtze, River Delta and the Pearl River Delta. *Int. J. Appl. Earth Obs. Geoinfor.* **2014,** *30*, 42-55.
58. Dahiya, B., Cities in Asia, 2012: Demographics, economics, poverty, environment and governance. *Cities* **2012,** *29*, S44-S61.
59. Wang, T.; Xue, L.; Brimblecombe, P.; Lam, Y. F.; Li, L.; Zhang, L., Ozone pollution in China: a review of concentrations, meteorological influences, chemical precursors, and effects. *Sci. Total Environ.* **2017,** *575*, 1582-1596.
60. Han, L.; Zhou, W.; Li, W.; Li, L., Impact of urbanization level on urban air quality: a case of fine particles ($PM_{2.5}$) in Chinese cities. *Environ. Pollut.* **2014,** *194*, 163-170.
61. Chang, Y.; Deng, C.; Dore, A. J.; Zhuang, G., Human excreta as a stable and important source of atmospheric ammonia in the megacity of Shanghai. *Plos One* **2015,** *10*, (12), e0144661.

62. Rumsey, I.; Cowen, K.; Walker, J.; Kelly, T.; Hanft, E.; Mishoe, K.; Rogers, C.; Proost, R.; Beachley, G.; Lear, G., An assessment of the performance of the Monitor for AeRosols and GAses in ambient air (MARGA): a semi-continuous method for soluble compounds. *Atmos. Chem. Phys.* **2014,** *14*, (11), 5639-5658.
63. Walters, W. W.; Goodwin, S. R.; Michalski, G., Nitrogen stable isotope composition ($\delta^{15}N$) of vehicle-emitted NO_x. *Environ. Sci. Technol.* **2015,** *49*, (4), 2278-2285.
64. Liu, D.; Fang, Y.; Tu, Y.; Pan, Y., Chemical method for nitrogen isotopic analysis of ammonium at natural abundance. *Anal. Chem.* **2014,** *86*, (8), 3787-92.
65. Chang, Y.; Liu, X.; Deng, C.; Dore, A. J.; Zhuang, G., Source apportionment of atmospheric ammonia before, during, and after the 2014 APEC summit in Beijing using stable nitrogen isotope signatures. *Atmos. Chem. Phys.* **2016,** *16*, (18), 11635-11647.
66. Hu, J.; Chen, J.; Ying, Q.; Zhang, H., One-year simulation of ozone and particulate matter in China using WRF/CMAQ modeling system. *Atmos. Chem. Phys.* **2016,** *16*, (16), 10333-10350.
67. Layman, C. A.; Araujo, M. S.; Boucek, R.; Hammerschlag-Peyer, C. M.; Harrison, E.; Jud, Z. R.; Matich, P.; Rosenblatt, A. E.; Vaudo, J. J.; Yeager, L. A.; Post, D. M.; Bearhop, S., Applying stable isotopes to examine food-web structure: an overview of analytical tools. *Biological Reviews* **2012,** *87*, (3), 545-562.
68. Ward, E. J.; Semmens, B. X.; Phillips, D. L.; Moore, J. W.; Bouwes, N., A quantitative approach to combine sources in stable isotope mixing models. *Ecosphere* **2011,** *2*, (2), 19.
69. Zong, Z.; Wang, X.; Tian, C.; Chen, Y.; Fang, Y.; Zhang, F.; Li, C.; Sun, J.; Li, J.; Zhang, G., First Assessment of NO_x sources at a regional background site in North China using isotopic analysis linked with modeling. *Environ. Sci. Technol.* **2017,** *51*, (11), 5923-5931.
70. Parnell, A. C.; Inger, R.; Bearhop, S.; Jackson, A. L., Source partitioning using stable isotopes: coping with too much variation. *Plos One* **2010,** *5*, (3), e9672.
71. Ward, E. J.; Semmens, B. X.; Schindler, D. E., Including source uncertainty and prior information in the analysis of stable isotope mixing models. *Environ. Sci. Technol.* **2010,** *44*, (12), 4645-4650.
72. Divers, M. T.; Elliott, E. M.; Bain, D. J., Quantification of nitrate sources to an urban stream using dual nitrate isotopes. *Environ. Sci. Technol.* **2014,** *48*, (18), 10580-10587.
73. Blumenthal, S. A.; Chritz, K. L.; Rothman, J. M.; Cerling, T. E., Detecting intraannual dietary variability in wild mountain gorillas by stable isotope analysis of feces. *Proc. Natl. Acad. Sci. U. S. A.* **2012,** *109*, (52), 21277-21282.
74. Rutz, C.; Bluff, L. A.; Reed, N.; Troscianko, J.; Newton, J.; Inger, R.; Kacelnik, A.; Bearhop, S., The ecological significance of tool use in new Caledonian crows. *Science* **2010,** *329*, (5998), 1523-1526.
75. Palacio, S.; Azorín, J.; Montserrat-Martí, G.; Ferrio, J. P., The crystallization water of gypsum rocks is a relevant water source for plants. *Nat. Commun.* **2014,** *5*, 4660.
76. Felix, J. D.; Elliott, E. M.; Gish, T. J.; McConnell, L. L.; Shaw, S. L., Characterizing the isotopic composition of atmospheric ammonia emission sources using passive samplers and a combined oxidation-bacterial denitrifier approach. *Rapid Commun. Mass Sp.* **2013,** *27*, (20), 2239-2246.
77. Chang, Y.; Ma, H., Comment on "Fossil fuel combustion-related emissions dominate atmospheric ammonia sources during severe haze episodes: Evidence from ^{15}N-stable isotope in size-resolved aerosol ammonium". *Environ. Sci. Technol.* **2016,** *50*, (19), 10765-10766.
78. Carslaw, D. C.; Beevers, S. D.; Ropkins, K.; Bell, M. C., Detecting and quantifying aircraft and other on-airport contributions to ambient nitrogen oxides in the vicinity of a large international airport. *Atmos. Environ.* **2006,** *40*, (28), 5424-5434.
79. Carslaw, D. C.; Ropkins, K., Openair — An R package for air quality data analysis. *Environ. Modell. Softw.* **2012,** *27*, 52-61.
80. Chang, Y.; Deng, C.; Cao, F.; Cao, C.; Zou, Z.; Liu, S.; Lee, X.; Li, J.; Zhang, G.; Zhang, Y., Assessment of carbonaceous aerosols in Shanghai, China – Part 1: long-term evolution, seasonal variations, and meteorological effects. *Atmos. Chem. Phys.*, **2017,** *17*, 9945-9964.
81. Chang, Y.; Huang, K.; Xie, M.; Deng, C.; Zou, Z.; Liu, S.; Zhang, Y., First long-term and near real-time measurement of trace elements in China's urban atmosphere: temporal variability, source apportionment and precipitation effect. *Atmos. Chem. Phys.*, **2018**, *18*, 11793-11812.
82. Meng, Z. Y.; Lin, W. L.; Jiang, X. M.; Yan, P.; Wang, Y.; Zhang, Y. M.; Jia, X. F.; Yu, X. L., Characteristics of atmospheric ammonia over Beijing, China. *Atmos. Chem. Phys.* **2011,** *11*, (12), 6139-6151.

83. Cao, J. J.; Zhang, T.; Chow, J. C.; Watson, J. G.; Wu, F.; Li, H., Characterization of Atmospheric Ammonia over Xi'an, China. *Aerosol Air Qual. Res.* **2009,** *9*, (2), 277-289.

84. Ju, X. T.; Xing, G. X.; Chen, X. P.; Zhang, S. L.; Zhang, L. J.; Liu, X. J.; Cui, Z. L.; Yin, B.; Christie, P.; Zhu, Z. L.; Zhang, F. S., Reducing environmental risk by improving N management in intensive Chinese agricultural systems. *Proc. Natl. Acad. Sci. U. S. A.* **2009,** *106*, (9), 3041-3046.

85. Wei, S.; Dai, Y.; Liu, B.; Zhu, A.; Duan, Q.; Wu, L.; Ji, D.; Ye, A.; Yuan, H.; Zhang, Q.; Chen, D.; Chen, M.; Chu, J.; Dou, Y.; Guo, J.; Li, H.; Li, J.; Liang, L.; Liang, X.; Liu, H.; Liu, S.; Miao, C.; Zhang, Y., A China data set of soil properties for land surface modeling. *J. Adv. Model. Earth Sy.* **2013,** *5*, (2), 212-224.

86. Zhao, X.; Xie, Y. X.; Xiong, Z. Q.; Yan, X. Y.; Xing, G. X.; Zhu, Z. L., Nitrogen fate and environmental consequence in paddy soil under rice-wheat rotation in the Taihu lake region, China. *Plant Soil* **2009,** *319*, (1), 225-234.

87. Kang, C. M.; Lee, H. S.; Kang, B. W.; Lee, S. K.; Sunwoo, Y., Chemical characteristics of acidic gas pollutants and $PM_{2.5}$ species during hazy episodes in Seoul, South Korea. *Atmos. Environ.* **2004,** *38*, (28), 4749-4760.

88. Gong, L.; Lewicki, R.; Griffin, R. J.; Flynn, J. H.; Lefer, B. L.; Tittel, F. K., Atmospheric ammonia measurements in Houston, TX using an external-cavity quantum cascade laser-based sensor. *Atmos. Chem. Phys.* **2011,** *11*, (18), 9721-9733.

89. Singh, S.; Kulshrestha, U. C., Abundance and distribution of gaseous ammonia and particulate ammonium at Delhi, India. *Biogeosci.* **2012,** *9*, (12), 5023-5029.

90. Singh, S.; Kulshrestha, U. C., Rural versus urban gaseous inorganic reactive nitrogen in the Indo-Gangetic plains (IGP) of India. *Environ. Res. Lett.* **2014,** *9*, (12), 125004.

91. Van Damme, M.; Clarisse, L.; Heald, C. L.; Hurtmans, D.; Ngadi, Y.; Clerbaux, C.; Dolman, A. J.; Erisman, J. W.; Coheur, P. F., Global distributions, time series and error characterization of atmospheric ammonia (NH_3) from IASI satellite observations. *Atmos. Chem. Phys.* **2014,** *14*, (6), 2905-2922.

92. Clarisse, L.; Clerbaux, C.; Dentener, F.; Hurtmans, D.; Coheur, P. F., Global ammonia distribution derived from infrared satellite observations. *Nat. Geosci.* **2009,** *2*, (7), 479-483.

93. Wang, S.; Nan, J.; Shi, C.; Fu, Q.; Gao, S.; Wang, D.; Cui, H.; Saiz-Lopez, A.; Zhou, B., Atmospheric ammonia and its impacts on regional air quality over the megacity of Shanghai, China. *Sci. Rep.* **2015,** *5*, (1), 15842.

94. Dewes, T., Effect of pH, temperature, amount of litter and storage density on ammonia emissions from stable manure. *J. Agri. Sci.* **2009,** *127*, (4), 501-509.

95. Tanner, P. A., Vehicle-related ammonia emissions in Hong Kong. *Environ. Chem. Lett.* **2009,** *7*, (1), 37-40.

96. Perrino, C.; Catrambone, M.; Di Bucchianico, A. D. M.; Allegrini, I., Gaseous ammonia in the urban area of Rome, Italy and its relationship with traffic emissions. *Atmos. Environ.* **2002,** *36*, (34), 5385-5394.

97. Hu, Q.; Zhang, L.; Evans, G. J.; Yao, X., Variability of atmospheric ammonia related to potential emission sources in downtown Toronto, Canada. *Atmos. Environ.* **2014,** *99*, 365-373.

98. Sommer, S. G.; Olesen, J. E.; Christensen, B. T., Effects of temperature, wind speed and air humidity on ammonia volatilization from surface applied cattle slurry. *J. Agri. Sci.* **2009,** *117*, (1), 91-100.

99. Cheng, H.; Hu, Y.; Reinhard, M., Environmental and Health Impacts of Artificial Turf: A Review. *Environ. Sci. Technol.* **2014,** *48*, (4), 2114-2129.

100. Asman, W. A.; Sutton, M. A.; Schjørring, J. K., Ammonia: Emission, atmospheric transport and deposition. *New Phytol.* **1998,** *139*, (1), 27-48.

101. Behera, S. N.; Sharma, M.; Aneja, V. P.; Balasubramanian, R., Ammonia in the atmosphere: a review on emission sources, atmospheric chemistry and deposition on terrestrial bodies. *Environ. Sci. Pullut. Res. Int.* **2013,** *20*, (11), 8092-8131.

102. Phillips, D. L.; Gregg, J. W., Source partitioning using stable isotopes: coping with too many sources. *Oecologia* **2003,** *136*, (2), 261-269.

103. Chang, Y.; Zhang, Y.; Tian, C.; Zhang, S.; Ma, X.; Cao, F.; Liu, X.; Zhang, W.; Kuhn, T.; Lehmann, M. F., Nitrogen isotope fractionation during gas-to-particle conversion of NO_x to NO_3^- in the atmosphere – implications for isotope-based NO_x source apportionment. *Atmos. Chem. Phys.* **2018,** *18*, (16), 11647-11661.

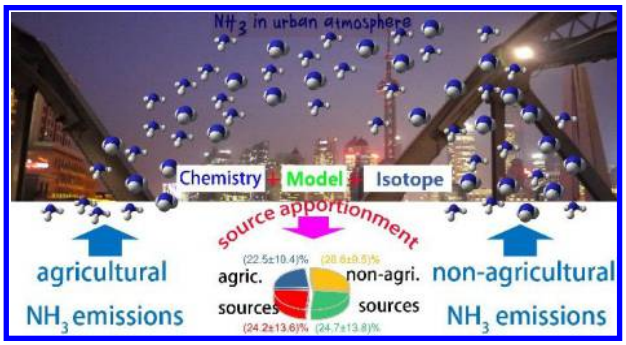

TOC art figure (8 cm*4.24 cm)

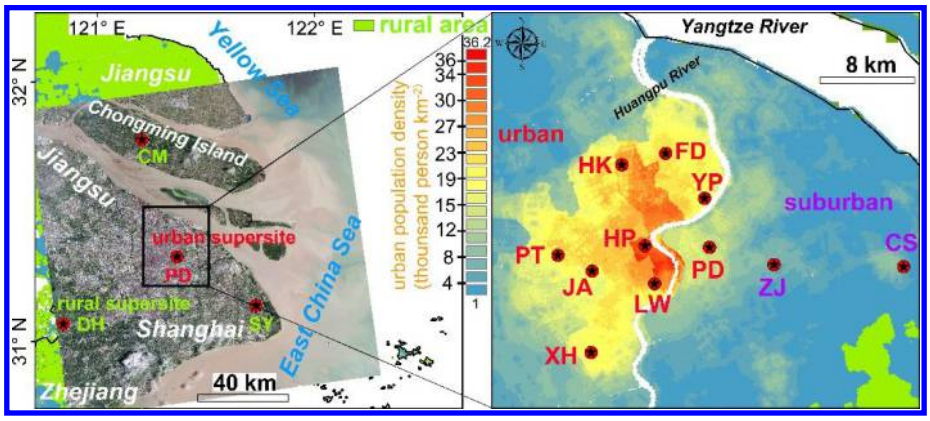

746

747 **Figure 1.** Shanghai passive ammonia monitoring network. The natural-

748 color satellite image in the left panel shows the urban area of Shanghai in 2016, along

749 with its major island Chongming. The right panel presents the population density in

750 Shanghai, which was retrieved from a newly released high-resolution (100 m × 100 m

751 per pixel) population map of China in 2010 (worldpop.org.uk).

752

753

754

755

756

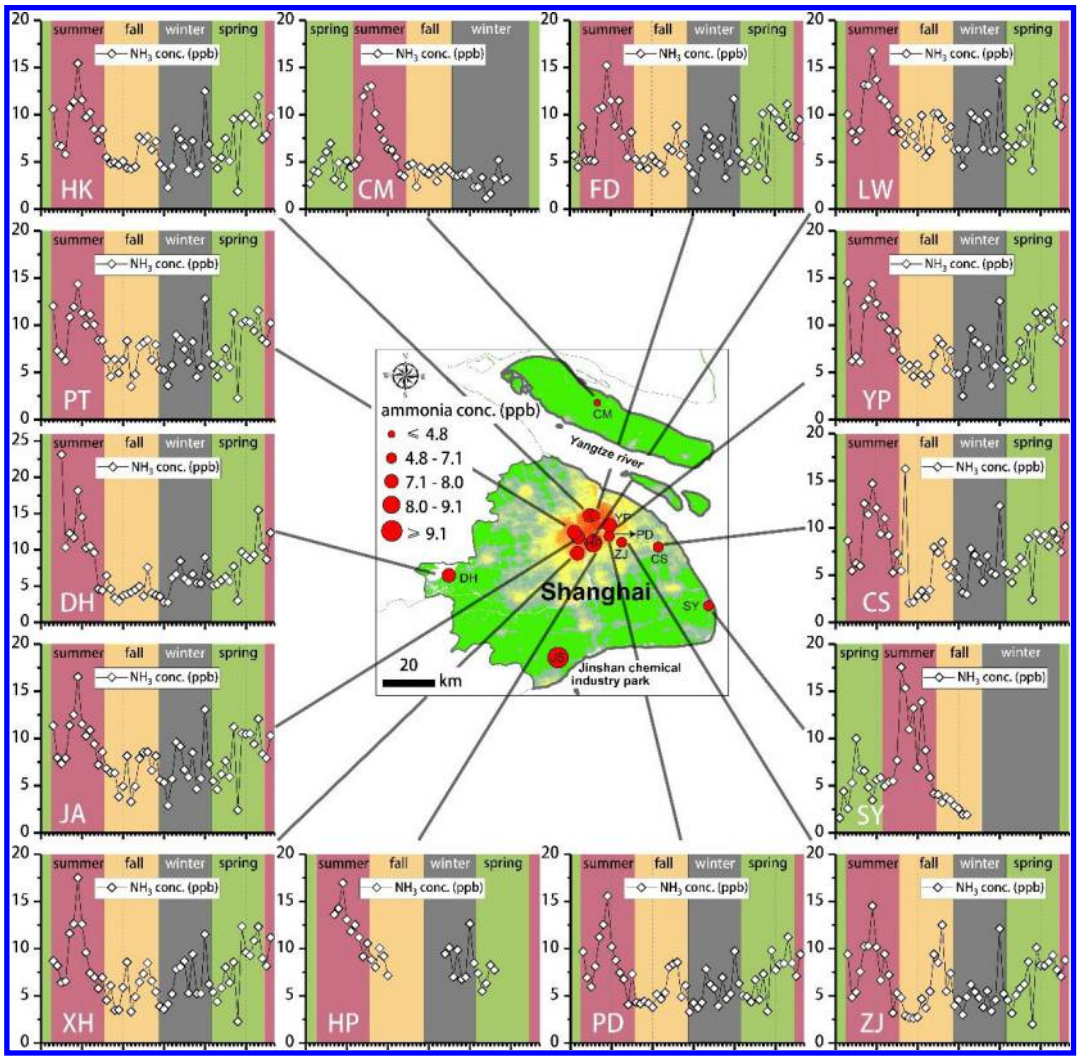

757

758 **Figure 2.** Sample-specific and group-averaged mixing ratios of ambient NH_3

759 measured with Ogawa passive samplers at fourteen surface locations in Shanghai.

760 Excepting the green color in the map (indicating rural areas), the color scheme is

761 population density with the scale the same as that in Fig. 1 (retrieved from

762 worldpop.org.uk).

763

764

765

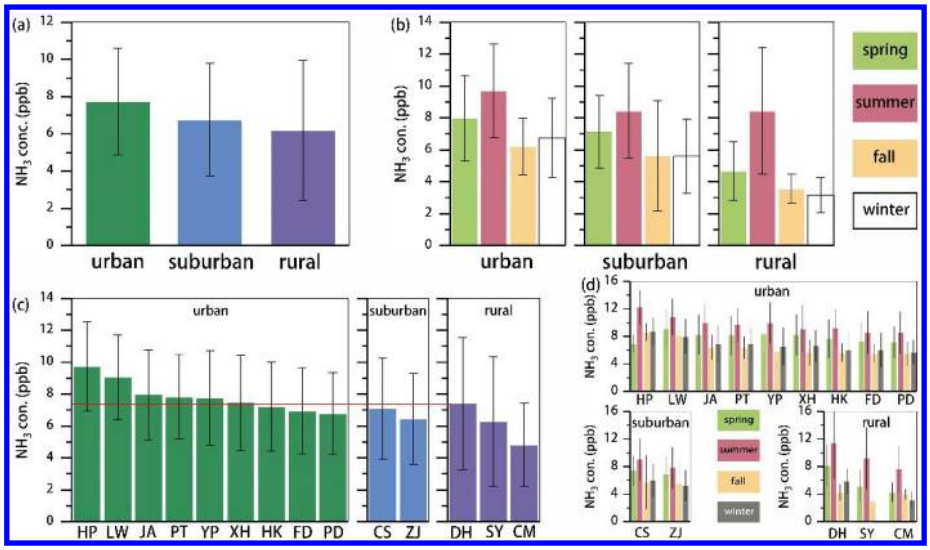

766

767 **Figure 3.** Comparison of the ambient NH_3 concentrations (mean ± 1σ) among (**a**)

768 different site types (urban/suburban/rural), (**b**) different seasons

769 (spring/summer/fall/winter) within a specific site type, (**c**) different individual sites, and

770 (**d**) different seasons (spring/summer/fall/winter) within a specific site.

771

772

773

774

775

776

777

778

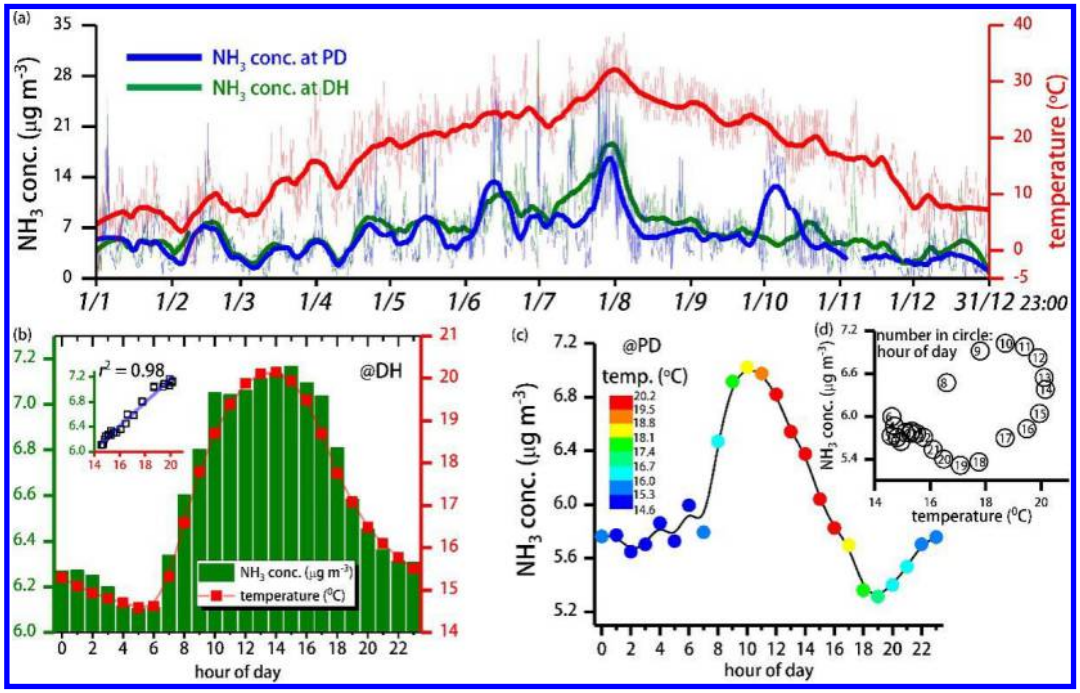

779

780 **Figure 4.** (**a**) Hourly variations of temperature (red) in Shanghai and NH_3
781 concentrations at the PD urban site (blue) and DH rural site (green), along with 500-
782 point Savitzky-Golay smoothed records from 1 January to 31 December 2015. (**b**)
783 Diurnal variation of NH_3 concentration and temperature and their correlation at DH rural
784 site in 2015. (**c**) Diurnal variation of NH_3 concentration (colored by temperature) at the
785 urban PD site in 2015. (**d**) Scatter plot of diurnal temperature and NH_3 concentration at
786 the urban PD site in 2015.

787

788

789

790

791

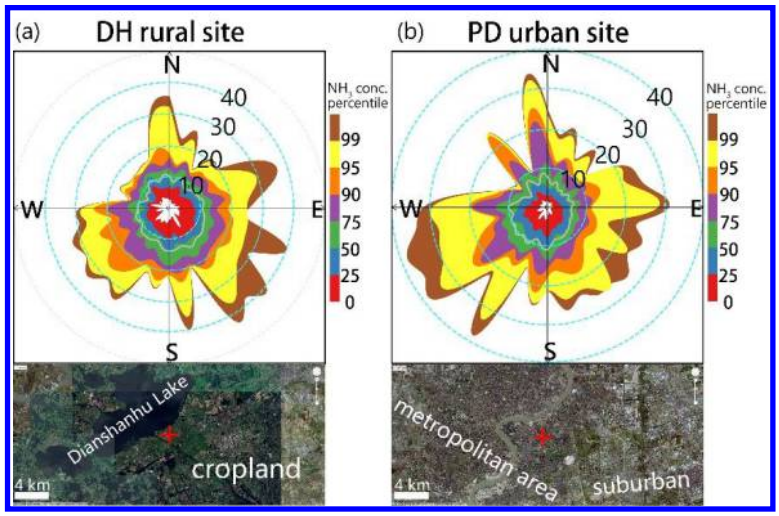

792

793 **Figure 5.** Bivariate polar plots (BPP) of the percentiles of NH_3 concentrations at (**a**)

794 rural DH site and (**b**) urban PD site. The natural-color satellite images below are the

795 land use maps corresponding to each site.

796

797

798

799

800

801

802

803

804

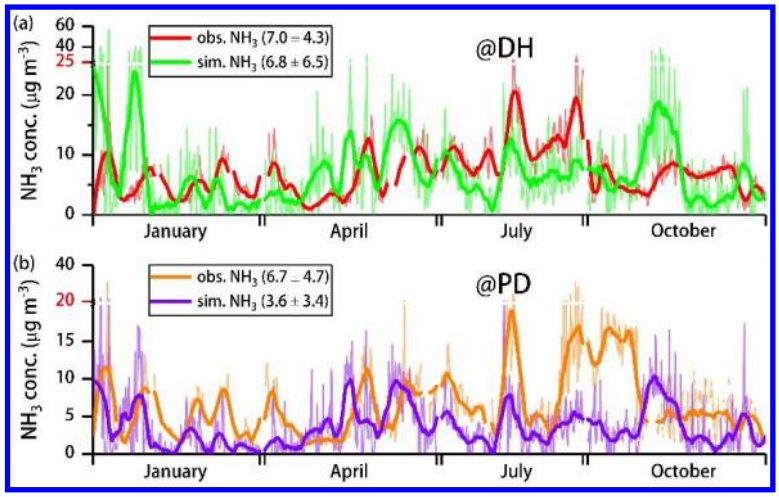

805

806 **Figure 6.** Comparison of hourly observed and simulated NH_3 concentrations at (**a**) DH

807 rural site and (**b**) PD urban site.

808

809

810

811

812

813

814

815

816

817

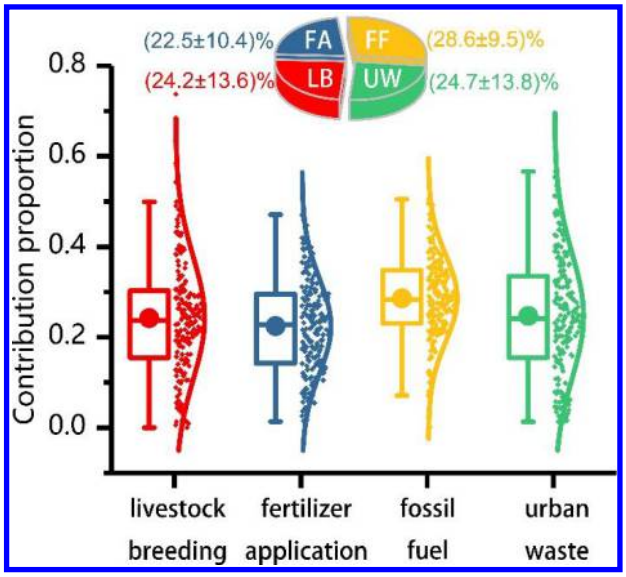

818

819 **Figure 7.** Isotope-based source apportionment of atmospheric NH_3 at PD urban site

820 with the normal distribution and variation range (within 5 and 95 percentiles).

821

822

823

824

825

826

827

828

829

830 **Table 1**. Mass concentrations and isotopic signatures ($\delta^{15}N$) of major NH_3 sources.

Category	sub-category	NH_3 (μg m^{-3})	δ^{15}N-NH_3 (‰)	N	reference
livestock breeding (LB)	pig breeding	462.2 to 1502.8	-31.7 to -27.1	7	[65]
N-fertilizer application (FA)	urea	165.6 to 623.7	-52.0 to -47.6	5	[65]
urban waste (UW)	solid waste	271.2 to 542.4	-37.6 to -29.9	8	[65]
	wastewater	127.2 to 258.5	-41.9 to -39.2	8	[65]
	human excreta	3238.0 to 6211.0	-39.6 to -37.3	8	[61]
fossil fuel-related (FF)	vehicle (road tunnel)	33.2 to 87.4	-17.8 to -9.6	8	[65]
	power plant (NH_3 slip)	not available	-14.6, -11.3	2	[76]

843

844

845

846

847

848 **Table 2.** Comparison of atmospheric NH_3 concentrations (in ppb) between urban and

849 suburban/rural areas in different regions.

location	period	average NH_3 concentration		reference
		urban	suburban/rural	
Shanghai, CN	2014.5-2015.6	7.8	6.8/6.2	this study
Xi'an, CN	2006.4-2007.4	18.6	20.3	[83]
Beijing, CN	2007.1-2010.7	22.8	10.2	[82]
Hong Kong, CN	2003.10-2006.5	10.2	0.2	[95]
Delhi, IN	2012.10-2013.9	52.8	65.6	[90]
Rome, IT	2001.5-2002.3	5.3	3.5	[96]
Toronto, CA	2003.7-2011.9	2.3-3.0	0.1-4	[97]

850

851

852

853